How Can a Focal Seizure Lead to a Dacrystic Behavior? A Case Analyzed with Functional Connectivity in Stereoelectroencephalography

Barbara Marx, Samuel Medina-Villalon, Fabrice Bartolomei, Stanislas Lagarde

How can a focal seizure lead to a dacrystic behavior? A case analyzed with functional connectivity in SEEG

Authors: Barbara Marx [a]; Samuel Medina-Villalon [a,b]; Fabrice Bartolomei [a,b]; Stanislas Lagarde [a,b]*

Affiliations:

[a] APHM, Timone Hospital, Epileptology Department, Marseille, France, Member of the ERN EpiCARE

[b] Aix Marseille University, INSERM, INS, Inst Neurosci Syst, Marseille, France

*** Corresponding author:**

Dr Stanislas Lagarde

Epileptology & Cerebral Rhythmology Department, University Hospitals of Marseille; Marseille, France

Stanislas.Lagarde@ap-hm.fr

Abstract

We present a case of a patient with focal non-motor emotional seizures with dacrystic expression in the context of drug-resistant Magnetic Resonance Imaging (MRI) negative epilepsy. The pre-surgical evaluation suggested a hypothesis of a right fronto-temporal epileptogenic zone. Stereoelectroencephalography (SEEG) recorded dacrystic seizures arising from the right anterior operculo-insular (*pars orbitalis*) area with secondary propagation to temporal and parietal cortices during the dacrystic behaviour. We analysed functional connectivity during the ictal dacrystic behaviour and found an increase of the functional connectivity within a large right fronto-temporo-insular network, broadly similar to the "emotional excitatory" network. It suggests that focal seizure, potentially, from various origins but leading to disorganization of these physiological networks may generate dacrystic behaviour.

Introduction

Among focal seizures with non-motor onset, some are mainly characterized by subjective and/or objective emotional content. These seizures are grouped as “emotional” in the International League Against Epilepsy (ILAE) classification of seizures types, and can include positive or negative emotion [1]. Amongst them, dacrystic seizures are characterized by paroxysmal manifestations of crying that include lacrimation, grimacing, sobbing, sad facial expression, yelling, with or without subjective feeling of sadness [2]. Dacrystic seizures may be observed in epilepsies associated with hypothalamic hamartoma but also in other types of focal epilepsies [2,3]. The underlying pathophysiology basis of this ictal behaviour is not well established. It has been hypothesized that a presumed ‘facio-respiratory control centre’ for emotional expression located in the brainstem is released from voluntary control in reported cases of cortical lesioning, or by inactivation by seizures [4]. It is known that several regions (prefrontal cortex, insula, cingulum, amygdala, striatum, hypothalamus, premotor/motor areas) are functionally connected to this centre and postulated that if a seizure alters the normal functioning of this network it could lead to dacrystic behaviour by a diaschisis phenomenon. However, no previous study has precisely investigated the modification of functional connectivity within this network during dacrystic seizures.

We took advantage of stereoelectroencephalography (SEEG) recordings to analyse functional connectivity changes during ictal dacrystic behaviour.

Case Description

We present the case of a 57-year-old right-handed man, with drug-resistant focal epilepsy and negative Magnetic Resonance Imaging (MRI). His seizures are characterized by an aura of the sensation of electrical discharges in the head, followed by crying behaviour with sad facial mimicry but without conscious emotion. Scalp video-electroencephalography (EEG) showed abundant interictal epileptiform discharges over the right fronto-temporal electrodes and ictal fast activity over the same electrodes. Magnetoencephalography (MEG) source imaging of abundant interictal spikes found generators within the right inferior frontal gyrus, anterior ventral insula and orbitofrontal cortex, and slow spikes coming from the right temporal lobe (superior temporal and temporal pole areas). Cerebral 18F-fluorodeoxyglucose – positron emission tomography (FDG-PET) showed hypometabolism affecting the right orbitofrontal, mesial prefrontal and anterior insular regions. At the end of this non-invasive assessment, we hypothesized a right fronto-temporo-insular epileptogenic network. Due to the absence of an epileptogenic lesion on MRI and suspicion of extra-temporal epilepsy, we performed a SEEG to accurately define the epileptogenic zone (EZ) [5].

Methods

1. SEEG recording

The number and the location of the SEEG electrodes were defined based on our clinical hypothesis. SEEG exploration was performed using intracerebral multiple-contact electrodes (Alcis), consisting of 10–15 contacts with length 2mm, diameter 0.8 mm, spaced by 1.5 mm[6].

Signals were recorded on a 256-channel Natus system, sampled at 512 Hz and recorded on a hard disk (16 bits/sample) using no digital filter. Two hardware filters were present in the acquisition procedure: a high-pass filter (cut-off frequency = 0.16 Hz at 3 dB), and an anti-aliasing low-pass filter (cut-off frequency = 170Hz). For the anatomical location of SEEG contacts, we co-registered pre-implantation cerebral MRI and post-implantation Computed Tomography (CT) (using the maximization of normalized mutual information and trilinear interpolation) using the GARDEL (graphical user interface (GUI), https://meg.univ-amu.fr/wiki/GARDEL:presentation)[7]. Long-term video-SEEG monitoring was performed to record several of the patient's habitual seizures, following a partial withdrawal of antiseizure medications. Bipolar electrical stimulations of adjacent SEEG contacts were performed to trigger the habitual aura or seizure and for functional mapping purposes (low frequency stimulation (1 Hz) for a continuous period of up to 40 s, and high frequency stimulation (50 Hz) during 2–5 s, with intensity ranging from 0.5 to 3 mA[8]).

2. Quantification of ictal activity

Interictal and ictal activities were firstly analysed visually using a bipolar montage. Then to define quantitatively the epileptogenic zone (EZ), we used the epileptogenicity index (EI). EI is a semi-automatic method to quantify the dynamic of the fast-activity genesis at seizure onset. The epileptogenicity index is based on two important features of the transition from pre-ictal to ictal activity: (i) the redistribution of signal energy from lower frequency bands (theta, alpha) toward higher frequency bands (beta, gamma); and (ii) the delay of appearance of these high frequencies. Briefly the EI quantifies the ability of each structure, involved in the

seizure, to generate ictal fast activity (above 12 Hz) with loss of background activity, and the precocity of this discharge regarding other structures [6].

3. Evaluation of SEEG signals disorganisation / entropy analyses

To select the channels for connectivity analyses disclosing a significant level of disorganization of their signals during dacrystic behaviour, we used "Permutation Entropy" (PE)[9]. PE considers the complexity of the electrophysiological signals, based on a measure of Shannon entropy of the relationships between neighbouring values of the time series. It gives a value between 0 and 1, 0 meaning that the signal is perfectly organized (for example in the case of a pure sine wave) and 1 completely disorganized (completely random noise). The algorithm used to apply PE on our data is the one developed by Unakafova and colleagues due to its algorithmic performance[10]. The parameters used were as follows: two-second window, one second steps, 0.1 second max lag, and 0.5 to 256 Hz filters. After calculation of PE, we applied a z-score normalization of the two periods (1: from electrical seizure onset to dacrystic behaviour onset, and 2: from dacrystic behaviour onset to electrical seizure offset) in comparison with the preictal period (baseline). To select channels with a statistically significant change in PE, we applied a Wilcoxon test comparing the PE values during the periods of interest with those during the baseline, with a Bonferroni correction.

4. Estimation of changes in brain functional connectivity

To estimate the changes in brain connectivity during dacrystic behaviour, we analysed the functional connectivity (FC) for the channels whose entropy was significantly modified using

non-linear correlation coefficient h^2. For each SEEG seizure, we selected two temporal periods for FC analysis: 1) pre-ictal period, segment selected until 5 seconds before the first SEEG ictal modification; and 2) period of dacrystic behaviour. Interdependencies between bipolar SEEG channels were estimated by pairwise nonlinear regression analysis based on the h^2 coefficient [11], using Anywave software (https://meg.univ-amu.fr/wiki/AnyWave)[12]. Nonlinear regression analysis aims to estimate the degree of association between two signals X and Y independently from the linear or nonlinear nature of this association. In a sliding window, a piecewise linear regression is performed between each pair of signals. The h^2 is the coefficient of determination, which measures the goodness of fit of the regression (equivalent to the r^2 used in linear regression). The h^2 is bounded between 0 (no correlation) and 1 (maximal correlation) and is asymmetric. This method has been shown to be particularly suitable for the analysis of EEG/SEEG signals in the context of epilepsy (review in [13]) and achieves high accuracy in the setting of intracranial EEG recordings [14]. We used a sliding window of 2 seconds with a step of 1 second and a maximum delay between signals of 100 ms. We used 0.5 Hz high pass and 256 Hz low pass filters for these analyses. To study FC changes, the z-score values of interactions comparing the different above-mentioned periods were obtained. We compared the connectivity during the ictal dacrystic behaviour with the pre-ictal period chosen before the electrical seizure onset.

Results of SEEG analysis

SEEG was performed with twelve right and two left electrodes (bilateral implantation because of negative-MRI), which covered the right temporal lobe, prefrontal cortex (especially orbitofrontal and cingulate), anterior insula and parietal lobe (lower part); and the left orbito-

158 frontal cortex (*Figure 1 and 2*). Interictal activity showed alteration of background activity with
159 abundant and repetitive spikes suggestive of focal cortical dysplasia (FCD) in anterior insula,
160 frontal operculum, and orbitofrontal areas. Six spontaneous seizures were recorded, five of
161 which with dacrystic behaviour. The seizure without dacrystic behaviour consisted only in an
162 aura without objective semiology and had similar SEEG onset but shorter duration and limited
163 propagation. Electrical stimulations of pars orbitalis (1 mA, 50 Hz) and anterior insular cortex
164 (2 mA, 50 Hz) triggered the usual aura of the patient without the dacrystic behaviour or
165 objective semiology.
166 All dacrystic seizures had similar seizure onset and propagation pattern both in term of
167 morphology of the discharges and of spatio-temporal organisation. A typical dacrystic seizure
168 is illustrated in the Figure 1. Seizure onset was characterized by a burst of polyspikes followed
169 by a low voltage fast activity within the contacts exploring orbitofrontal (almost all contacts
170 of electrode R), frontal operculum (lateral contacts of R and OF, intermediate contacts of Ia),
171 and anterior insula (mesial contacts of Ia and Im) areas. About 10 seconds after onset, the
172 discharge slowed to an alpha sinusoidal discharge in some previously involved structures and
173 propagated following a similar morphology to right hippocampus (mesial contacts of B), right
174 neocortical temporal regions (lateral contacts of A and B), right precuneus (mesial contacts of
175 PI) and right parietal lateral cortex (lateral contacts of PI). The dacrystic behaviour started 5
176 seconds after the installation of the sinusoidal alpha discharge, therefore 15 seconds after
177 seizure onset. At that time, we observed: 1) low voltage fast activity in right orbitofrontal (R),
178 second short gyrus of the anterior insula (mesial contacts of Im) and frontal operculum (OF);
179 2) sinusoidal alpha discharges in right hippocampus (mesial contacts of B), temporal neocortex
180 (lateral contacts of A and B), first short gyrus of anterior insula (mesial contacts of Ia),
181 precuneus (mesial contacts of PI) and lateral parietal cortex (lateral contacts of PI); 3) there

were no clear rhythmic or sinusoidal discharge but a modification of background activity with decrease of amplitude, decrease of low frequencies and increase of high frequency content, in the left frontal regions (orbito-frontal cortex: OR' and superior frontal cortex: CR'), and right dorsolateral prefrontal cortex (last contacts of CR and OR).

Using the EI to quantify the epileptogenicity of structures during seizures, an orbitofrontal (R), pars orbitalis (lateral R) and triangularis (lateral OF), anterior insula (Ia) and pars opercularis (Ia and OF) the epileptogenic zone (EZ) was delineated (*Figure 1*). The patient was operated with a tailored fronto-insular cortectomy without postoperative complication and is currently seizure-free for nine months. Histology confirmed a FCD type Ic.

Using PE to estimate the level of electrophysiological signals disorganization, we observed during the dacrystic behaviour a combination of 1) decreased signal complexity in a large network including the bilateral orbitofrontal cortices, anterior insula, hippocampus, and precuneus; 2) increased signal complexity in the frontal operculum and middle frontal gyrus (*Supplementary Figure*).

Using h^2 coefficient to estimate the modification of FC, we observed an increased connectivity within a large network including the EZ (right anterior insula, frontal operculum, and lateral orbitofrontal cortex) but also remote areas: right orbito-ventro-mesial, right prefrontal dorsolateral (superior and middle frontal gyri), right precuneus, right hippocampus and left orbito-ventro-mesial and superior frontal cortices (*Figure 2*).

Discussion

From a physiological point of view, dacrystic / crying behaviours are postulated to involve a complex system, composed of an "excitatory emotional" network (especially prefrontal

cortex, insular, cingulum and amygdala, as well as subcortical structures such as the striatum, hypothalamus, midbrain and pons), and an “inhibitory voluntary” network (mainly the premotor/motor areas for facial control) which interact with the periaqueductal grey matter, itself responsible for control/ coordination of facial expressions, breathing and vocalization during crying. It is hypothesized that pathological crying occurs when both excitatory and inhibitory networks are dysfunctional (“two hits theory”)[15]. In our case, we observed an increase of the functional connectivity within a large right fronto-temporo-insular network, broadly similar to the "emotional excitatory" network described above. It suggests that a focal seizure leading to the disorganization of functional connectivity within large network involved in crying may generate this behaviour during a seizure. A similar mechanism has already been reported in other complex behaviour observed during focal seizure such as humming automatisms [16].

Dacrystic seizures can be observed in epilepsies related to hypothalamic hamartomas (often associated with gelastic seizures), but also in focal epilepsies (especially temporal)[2]. Previous cases explored with intracerebral EEG showed propagation of the ictal discharge to the medial frontal structures at the time of dacrystic behaviour [17,18]. Moreover, crying behaviour has also been reported following electrical stimulation of the orbitofrontal cortex, the internal capsule and the anterior insula[19]. These data suggest that rather than a specific zone that would cause this behaviour, seizure-related dysfunction of a large number of functionally connected brain areas within an emotional network may lead to ictal emotional behaviour.

One of the limitations of our study is the limited sampling of contralateral temporo-parieto-insular regions and subcortical structures, due to obvious clinical limitations in the number of SEEG electrodes implanted. We report only one patient, and future studies on more patients analysed invasively and non-invasively (EEG) would be interesting.

Conclusion

Dacrystic behaviour can be seen in focal seizures. This probably does not correspond to the dysfunction of a unique structure but is rather related to the disorganization of connectivity within a large fronto-temporo-insular networks associated with the circuit involved in the physiology of crying. This disorganization may be triggered by the seizure itself or by electrical stimulation, affecting regions strongly connected to these circuits.

References

1. Fisher RS, Cross JH, French JA, et al. Operational classification of seizure types by the International League Against Epilepsy: Position Paper of the ILAE Commission for Classification and Terminology. Epilepsia. 2017;58:522–530.
2. Blumberg J, Fernández IS, Vendrame M, et al. Dacrystic seizures: Demographic, semiologic, and etiologic insights from a multicenter study in long-term video-EEG monitoring units. Epilepsia. 2012;53:1810–1819.
3. Espino PH, Burneo JG. Dacrystic seizures in MRI-negative patients. Epileptic Disord. 2022;24:427–430.
4. Wild B, Rodden FA, Grodd W, Ruch W. Neural correlates of laughter and humour. Brain. 2003;126:2121–2138.
5. Isnard J, Taussig D, Bartolomei F, et al. French guidelines on stereoelectroencephalography (SEEG). Neurophysiol Clin. Elsevier Masson SAS; Epub 2017.
6. Bartolomei F, Chauvel P, Wendling F. Epileptogenicity of brain structures in human temporal lobe epilepsy: A quantified study from intracerebral EEG. Brain. 2008;131:1818–1830.
7. Medina Villalon S, Paz R, Roehri N, et al. EpiTools, A software suite for presurgical brain mapping in epilepsy: Intracerebral EEG. J Neurosci Methods. Elsevier B.V.; 2018;303:7–15.
8. Trebuchon A, Racila R, Cardinale F, et al. Electrical stimulation for seizure induction during SEEG exploration: A useful predictor of postoperative seizure recurrence? J Neurol Neurosurg Psychiatry. 2021;92:22–26.
9. Bandt C, Pompe B. Permutation entropy: a natural complexity measure for time

271 series. Phys Rev Lett. Phys Rev Lett; 2002;88:4.
272 10. Unakafova V, Keller K. Efficiently Measuring Complexity on the Basis of Real-World
273 Data. Entropy. 2013;15:4392–4415.
274 11. Wendling F, Bartolomei F, Bellanger JJ, Chauvel P. Interpretation of interdependencies
275 in epileptic signals using a macroscopic physiological model of the EEG. Clin
276 Neurophysiol. 2001;112:1201–1218.
277 12. Colombet B, Woodman M, Badier JM, Bénar CG. AnyWave: A cross-platform and
278 modular software for visualizing and processing electrophysiological signals. J
279 Neurosci Methods. 2015;242:118–126.
280 13. Bartolomei F, Lagarde S, Wendling F, et al. Defining epileptogenic networks:
281 Contribution of SEEG and signal analysis. Epilepsia. 2017;58:1131–1147.
282 14. Wang HE, Bénar CG, Quilichini PP, Friston KJ, Jirsa VK, Bernard C. A systematic
283 framework for functional connectivity measures. Front Neurosci. 2014;8:1–22.
284 15. Klingbeil J, Wawrzyniak M, Stockert A, et al. Pathological laughter and crying: insights
285 from lesion network-symptom-mapping. Brain. 2021;144:3264–3276.
286 16. Bartolomei F, Wendling F, Vignal JP, Chauvel P, Liégeois-Chauvel C. Neural networks
287 underlying epileptic humming. Epilepsia. 2002;43:1001–1012.
288 17. Hogan RE, Rao VK. Hemifacial motor and crying seizures of temporal lobe onset: case
289 report and review of electro-clinical localisation. J Neurol Neurosurg Psychiatry.
290 2006;77:107–110.
291 18. Luciano D, Devinsky O, Perrine K. Crying seizures. Neurology. Neurology;
292 1993;43:2113–2117.
293 19. Burghardt T, Basha MM, Fuerst D, Mittal S. Crying with sorrow evoked by
294 electrocortical stimulation. Epileptic Disord. 2013;15:72–75.

295

Figure Legends

Figure 1:

A. Representation on the patient's 3 dimensions (3D) mesh of the mean epileptogenicity index (EI) across seizures.

A electrode explored amygdala (mesial part) and middle temporal gyrus (lateral part); B hippocampus and middle temporal gyrus; T: superior temporal gyrus; H: pulvinar, posterior insula and Heschl gyrus; PI: precuneus and supramarginal gyrus; R: orbito-frontal and pars orbitalis; OR orbito-frontal and middle frontal gyrus; OF: anterior insula and pars triangularis; CC: anterior cingulum and middle frontal gyrus; Ia: anterior insula and middle frontal gyrus; Im: middle insula and lateral premotor cortex.

B. 30 seconds of stereoelectroencephalography (SEEG) recording showing the seizure onset and the beginning of dacrystic behaviour associated to a propagation of the ictal discharge to the orbito-frontal cortex and anterior insula.

The entire SEEG page has a duration of 30 seconds, there is one second between each yellow vertical line, and the exact timing is indicated by the blue numbers at the top of the SEEG trace.

Figure 2:

Representation on the patient's 3 dimensions (3D) mesh of the changes in entropy during the dacrystic period (z-score compared to pre-ictal period illustrated by the sphere on each channel) and the change in functional connectivity (z-score compared to pre-ictal period illustrate by the links between channels).

A electrode explored amygdala (mesial part) and middle temporal gyrus (lateral part); B hippocampus and middle temporal gyrus; T: superior temporal gyrus; H: pulvinar, posterior insula and Heschl gyrus; PI: precuneus and supramarginal gyrus; R: orbito-frontal and pars orbitalis; OR orbito-frontal and middle frontal gyrus; OF: anterior insula and pars triangularis; CC: anterior cingulum and middle frontal gyrus; Ia: anterior insula and middle frontal gyrus; Im: middle insula and lateral premotor cortex.

Supplementary Figure Legend:

Boxplot of each change of entropy for each channel during dacrystic or preictal periods (z-score compared to pre-ictal period). The coloured ones are statistically significant, blue means a decrease and red an increase.

A

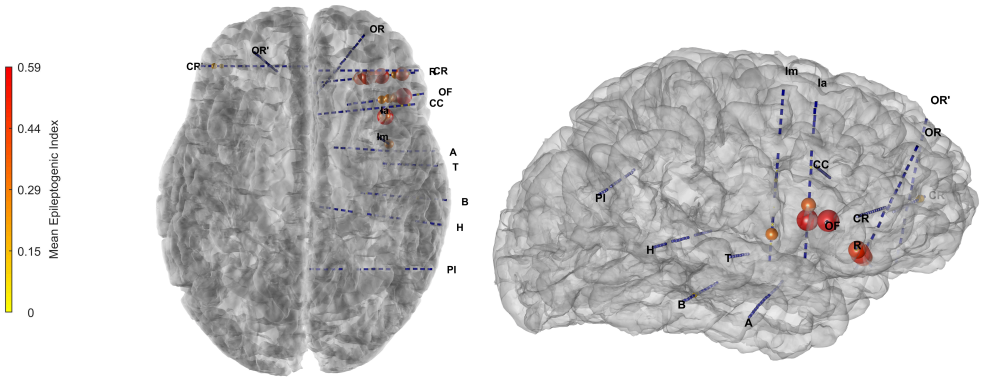
0.59
0.44
0.29
0.15
0
Mean Epileptogenic Index
OR
QR'
CR
FCR
OF
CC
Im
A
T
B
H
PI
Im
Ia
OR'
OR
CC
PI
OF
CR
H
T
B
A

B

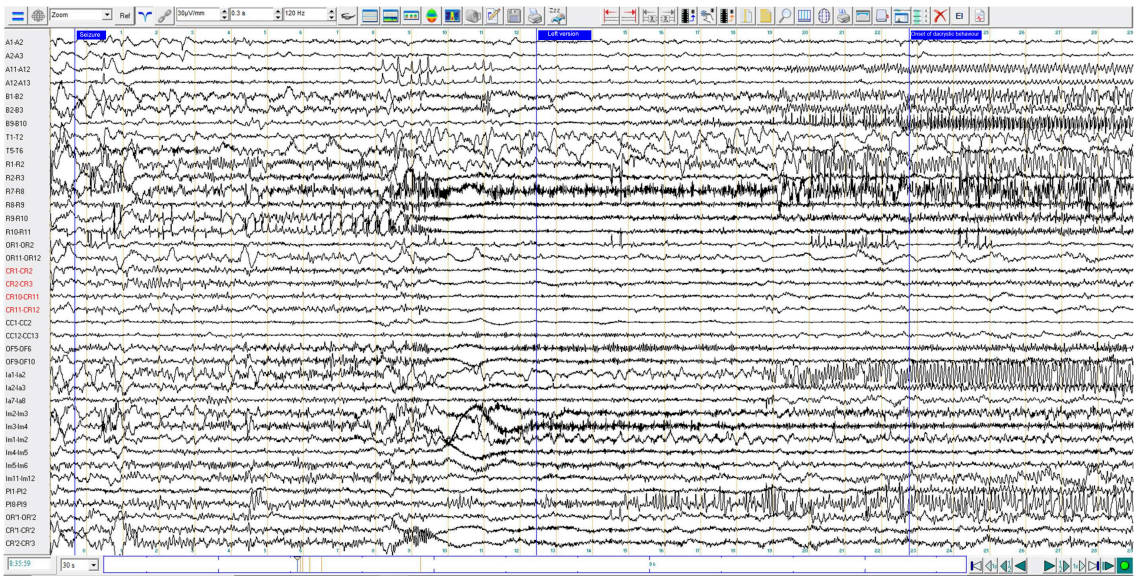
Seizure
Left version
Onset of diazepam behaviour
A1-A2
A2-A3
A11-A12
A12-A13
B1-B2
B2-B3
B9-B10
T1-T2
T5-T6
R1-R2
R2-R3
R7-R8
R8-R9
R9-R10
R10-R11
OR1-OR2
OR11-OR12
CR1-CR2
CR2-CR3
CR10-CR11
CR11-CR12
CC1-CC2
CC12-CC13
OF5-OF6
OF9-OF10
Ia1-Ia2
Ia2-Ia3
Ia7-Ia8
Im2-Im3
Im3-Im4
Im1-Im2
Im4-Im5
Im5-Im6
Im11-Im12
PI1-PI2
PI8-PI9
OR1-OR2
CR1-CR2
CR2-CR3

A

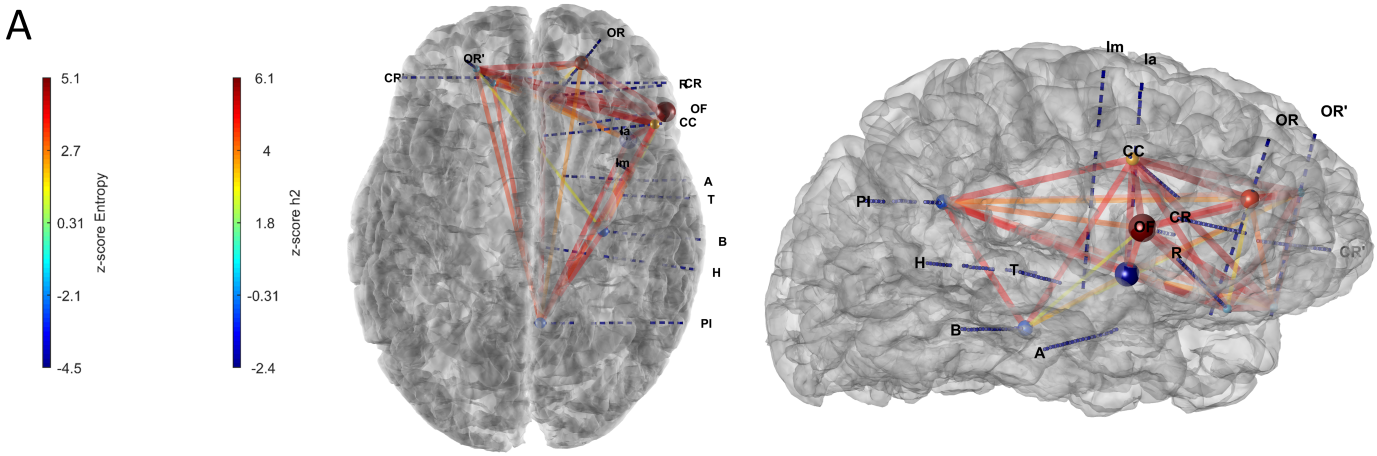
5.1
2.7
0.31
-2.1
-4.5
z-score Entropy
6.1
4
1.8
-0.31
-2.4
z-score h2
OR
OR'
CR
rCR
OF
CC
la
km
A
T
B
H
Pl
lm
la
OR
OR'
CC
Pl
CR
OF
R
H
T
CR'
B
A

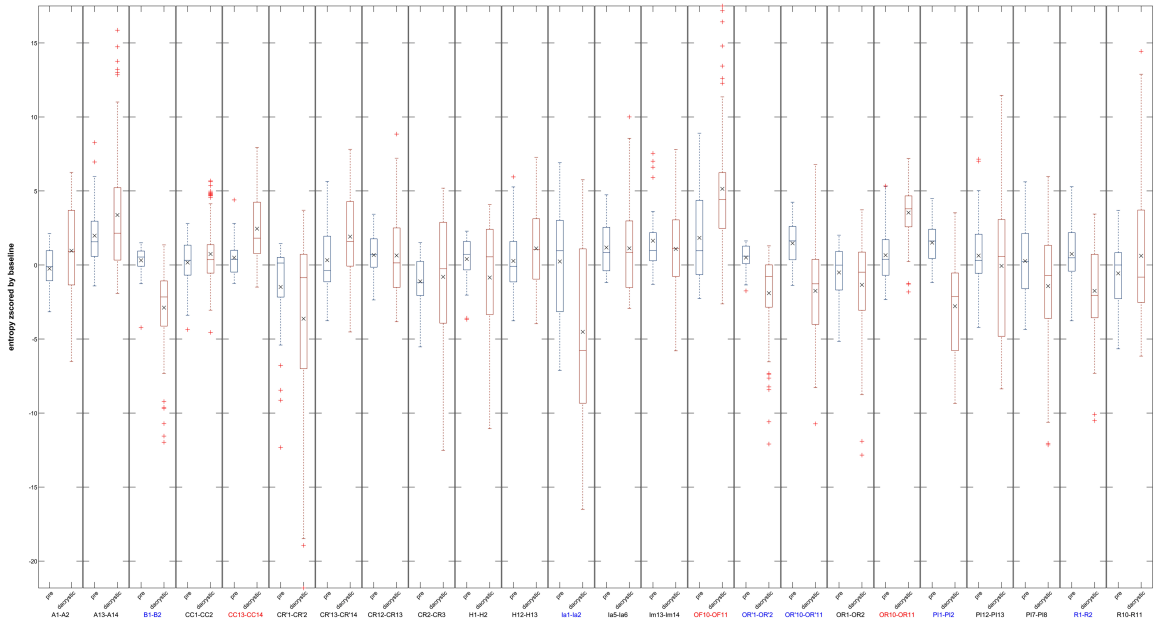
entropy zscored by baseline
15
10
5
0
-5
-10
-15
-20
pre
dasynbic
A1-A2
A13-A14
B1-B2
CC1-CC2
CC13-CC14
CR1-CR2
CR13-CR14
CR12-CR13
CR2-CR3
H1-H2
H12-H13
Ia1-Ia2
Ia5-Ia6
Im13-Im14
OF10-OF11
OR1-OR2
OR10-OR11
OR1-OR2
OR10-OR11
P1-P12
P12-P13
P7-P8
R1-R2
R10-R11